Appl. Phys. B (2016) 122:163
DOI 10.1007/s00340-016-6441-9

Applied Physics B
Lasers and Optics

Orthogonally polarized dual-wavelength Yb:KGW laser induced by thermal lensing

Haitao Zhao[1] · **Arkady Major**[1]

Received: 10 February 2016 / Accepted: 11 May 2016 / Published online: 27 May 2016
© Springer-Verlag Berlin Heidelberg 2016

Abstract Simultaneous dual-wavelength laser oscillation with orthogonal polarizations has been observed and analyzed in a continuous wave N_g-cut Yb:KGW oscillator. Without inserting any optical elements for polarization control, the N_m- and N_p-polarized modes, each of which possessed a distinct wavelength, coexisted and switched twice in two power regimes as the pump power was varied. The two wavelengths and their separation slightly depended on output coupling level. The wavelength switching and coexistence was studied and explained by considering the thermal and spectral anisotropy of the Yb:KGW crystals, which led to polarization-dependent reabsorption loss in the unpumped regions of the crystal. The maximum average output power obtained in the dual-wavelength regime was 4.6 W.

1 Introduction

Over the past years, there has been increasing research attention devoted to the development of dual-wavelength rare-earth-doped solid-state oscillators. Such operation regime benefits from the diverse energy transitions in rare-earth ions. For example, Nd-ions exhibit multiple sharp fluorescence peaks, allowing simultaneous emission of two wavelengths either with wide separation (e.g., 914 and 1064 nm) originating from the transitions between the excited manifold and different terminal manifolds or with narrow separation (e.g., 1086 and 1089 nm) resulting from transitions between the sublevels of two particular manifolds [1–5]. In contrast, Yb-ions have broad fluorescence spectra due to their relatively strong interactions between the electronic $^4F_{5/2}$–$^4F_{7/2}$ transitions and the host lattice vibrations. This makes them particularly attractive for generating dual-wavelength radiation with tunable separation in the THz region and further generating of THz waves through nonlinear frequency mixing. The THz waves, with their advantageous features over microwaves and infrared waves, have found numerous applications in biomedical imaging, nondestructive detection, and environmental monitoring [6–8]. The first dual-wavelength lasing from the Yb-ions, to the best of our knowledge, was observed in a Yb:$Sr_5(VO_4)_3F$ oscillator, where a fixed lasing wavelength at 1044 nm and a tunable one between 1113 and 1120 nm were obtained simultaneously [9]. Later, dual-wavelength lasing was reported from oscillators based on many other Yb-doped crystals such as Yb:$GdVO_4$, Yb:$YCa_4O(BO_3)_3$, Yb:$GdCa_4O(BO_3)_3$, Yb:$GdAl_3(BO_3)_4$, Yb:$KGd(WO_4)_2$, Yb:$CaGdAlO_4$, and Yb:$KLu(WO_4)_2$ [10–17].

The key factor that underlies the dual-wavelength lasing is the equalization of the net gain of the involved transitions which usually have different gain cross sections. It can be realized by incorporating wavelength-dependent or polarization-dependent optical elements to introduce different losses to separate transitions. In Nd-doped solid-state oscillators, for instance, two output couplers with different transmissions, a tilted etalon or a polarization beam splitter has been successfully employed [3–5]. By inserting two etalons, the dual-wavelength lasers with tunable separation in the range of 0–11 nm have been demonstrated in an Yb:KGW oscillator [14]. Similarly, in another Yb:KGW oscillator, two wavelengths in the ranges of 1020–1033 and 1033–1047 nm were generated simultaneously as two

✉ Arkady Major
a.major@umanitoba.ca

[1] Department of Electrical and Computer Engineering, University of Manitoba, 75A Chancellors Circle, Winnipeg, MB R3T 5V6, Canada

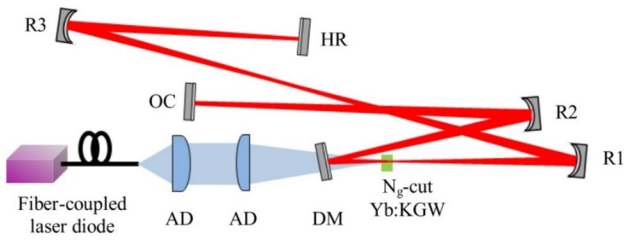

Fig. 1 Experimental layout of the cw dual-wavelength Yb:KGW oscillator. HR is the highly reflective mirror. *AD* is the achromatic doublet. *OC* is the output coupler. *R1*, *R2,* and *R3* are the concave mirrors with radii of curvature of 600, 600, and 750 mm, respectively

chirped volume Bragg gratings were inserted, leading to a tunable wavelength separation between 0 and 27 nm [15]. In both of these cases, however, the involved two lasing transitions occurred in two spatially separated regions of the crystal, which required complicated pumping and lasing configurations. A similar strategy can also be found in an Yb:$GdAl_3(BO_3)_4$ oscillator [13]. Recently, the use of an intracavity birefringent plate for dual-wavelength generation was also reported [18]. Practically, it would be desirable to achieve dual-wavelength lasing with a more simple configuration. Although this has been reported in many Yb-doped oscillators [10–12], the mechanism behind the equalization of the net gain at the two lasing wavelengths was not clearly identified yet.

In this work, we report a dual-wavelength lasing with the N_m- and N_p-polarizations in a simple diode-pumped Yb:KGW solid-state oscillator without inserting any extra optical elements for wavelength or polarization control. The two lasing wavelengths could be tuned slightly by using output couplers with different transmissions. A detailed investigation of the spatial matching between the pump and laser modes inside the gain medium revealed that the net gain equalization at the two wavelengths was caused by the polarization-dependent thermal lensing and reabsorption loss of the reshaped laser modes in the unpumped regions of the gain medium.

2 Experimental setup

The dual-wavelength lasing was observed in a delta cavity shown in Fig. 1. The AR-coated, 1.5 at.% doped Yb:KGW crystal (Eksma) had a slab geometry with 5 mm × 8 mm × 1.2 mm dimensions. The crystal was cut along the N_g-axis (5 mm), which allowed the produced laser radiation to be polarized along the N_m-axis (8 mm) and N_p-axis (1.2 mm). The crystal was wrapped in indium foil, and both 5 × 8 mm^2 faces were sandwiched in a copper cooling holder with circulating water held at 16 °C. The pump source was a fiber-coupled diode laser (with 100 μm core diameter and 0.22 NA) with maximum output power of 30 W and emission wavelength of 978–980 nm, depending on the output power level. This wavelength range corresponded to the pump absorption of 50–60 %. The pump mode was reimaged onto the crystal through two AR-coated achromatic doublets and a dichroic mirror with high transmission (>95 %) at the pump wavelength and high reflection (>99.9 %) in the 1020- to 1080-nm region, forming a waist of 300 μm in diameter at the center of the crystal. Several output couplers with transmissions in the range between 1.6 and 5 % were used. All other laser cavity mirrors were HR-coated (highly reflective, >99.9 %, Laseroptik GmbH) at lasing wavelength. The end HR mirror was placed on a micrometer-driven translation stage in order to finely adjust the size of the laser mode inside the crystal. Within the translation distance of 20 mm, the laser mode radius could be adjusted within the 190- to 235-μm range without considering the thermal lensing effect of the crystal. The thermal lensing was estimated to reshape the laser mode to have a better spatial matching with the pump mode as the pump power was increased.

3 Results and discussion

By placing a polarization beam splitter (>99.5 % transmission for the N_m-polarized mode and >95 % reflection for the N_p-polarized mode) after the output coupler (not shown in Fig. 1), the polarization state of the produced laser radiation could be determined. The measured output power for the N_m- and N_p-polarized modes as well as their sum against the pump power is shown in Fig. 2. The lasing threshold was reached as the pump power was increased to 10.5, 12 and 12.5 W for the output couplers with transmissions of 1.6, 3 and 5 %, respectively. This corresponded to the absorbed pump power of about 4.9, 5.8 and 6 W for the three output couplers, respectively. Compared to our previous results [19], the higher pump power at lasing threshold indicated spatial mismatch between the pump and laser modes in the gain medium and therefore the presence of additional reabsorption losses in the unpumped regions. This was demonstrated experimentally by measuring the thermal lensing using the modified beam propagation technique [20] and the size of the laser modes inside the gain medium. Among the three output couplers, the 5 % output coupler generated the highest output power of 4.6 W at the pump power of 26.8 W.

In the vicinity of the threshold pump powers, the laser was linearly polarized along the N_p-axis. For the 1.6 % output coupler (Fig. 2a), the polarization state was unchanged until the pump power was increased to 17.6 W, where the N_m-polarized mode appeared. The N_m- and N_p-polarized modes coexisted in a relatively narrow power range, in

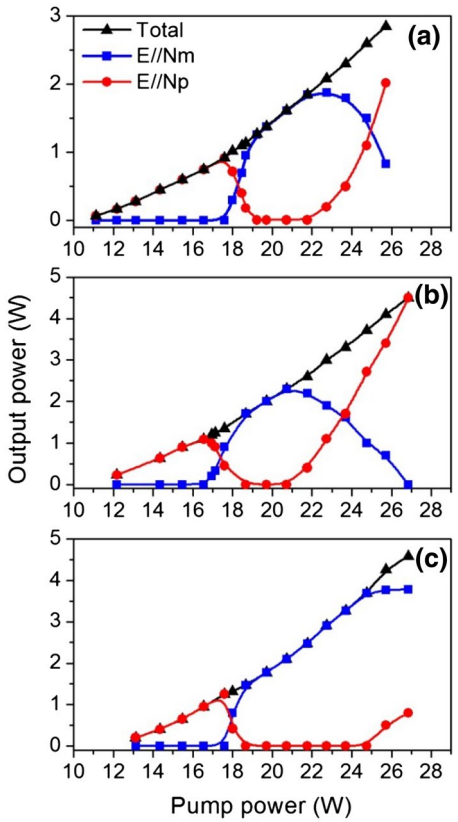

Fig. 2 The output power for the N_m- and N_p-polarized modes and the total output power against the pump power for output coupler transmissions of 1.6 % (**a**), 3 % (**b**), and 5 % (**c**)

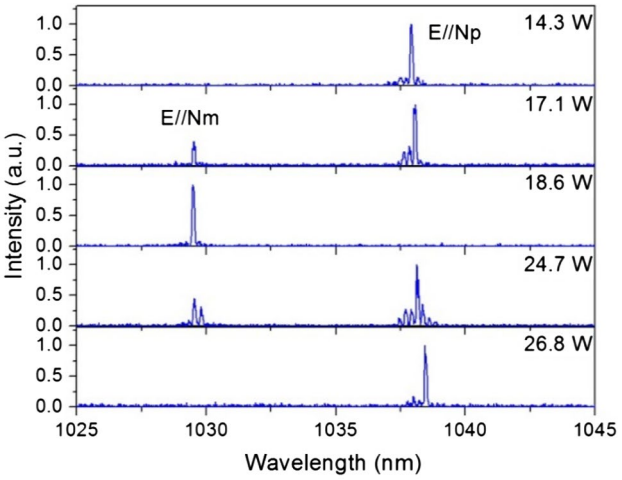

Fig. 3 The lasing spectra at different pump powers for the 3 % output coupling

Table 1 Lasing wavelengths for different output couplers

Output coupler transmission (%)	λ_m (nm) ($E//N_m$)	λ_p (nm) ($E//N_p$)	$\Delta\lambda$ (nm)
1.6	1030.5	1038.4	7.9
3	1029.5	1038.1	8.6
5	1028.7	1037.5	8.8

Measured in the second dual-wavelength lasing power range

which they had a similar net gain. A complete switching between the two modes was accomplished at 19.2 W leaving only the N_m-polarized mode to oscillate in the cavity. Interestingly enough, as the pump power was further increased to 21.8 W, the N_p-polarized mode reappeared. At this time, the coexistence between the N_m- and N_p-polarized modes occurred in a wider power range. Similar laser performance with polarization switching and coexistence could also be obtained for two other output couplers with 3 and 5 % transmissions (Fig. 2b, c, respectively). Correspondingly, the end HR mirror had to be translated a few millimeters away from the concave mirror R3. Such movement allowed the reduction of the laser mode size in the crystal and further reduction of the reabsorption losses (induced by the mode mismatching) introduced to the N_m- and N_p-polarized laser modes. The reappearance of the N_p-polarized mode for the 5 % output coupling happened at the higher pump power of 24.7 W. The complete switching between the two modes is believed to occur again with further increase of the pump power.

Due to the spectral anisotropy of the Yb:KGW crystals, the N_m- and N_p-polarizations exhibit distinct lasing wavelengths. The evolution of the lasing spectrum with the pump power for the 3 % output coupler is shown in Fig. 3. For the N_p-polarized mode, the wavelength initially appeared at 1037.9 nm and slightly shifted to the longer one as the pump power was increased. For the N_m-polarized mode, in contrast, the wavelength appeared at 1029.5 nm and little change was observed with the increase of the pump power. In the dual-wavelength operation regime, their spectral separation of ~8.6 nm was obtained. The lasing wavelengths for the N_m- and N_p-polarized modes which oscillated with different output coupler transmissions are summarized in Table 1. A modest tunability of the two wavelengths as well as their separation can be observed. This behavior can be explained by the loss-dependent spectral position of the peak gain in the broadband quasi-three-level gain media [19].

The observed switching and coexistence of the N_m- and N_p-polarized modes was attributed to the competition and equalization of their net gain. In order to investigate the mechanism behind this, we measured the thermal lensing and the spatial matching between the pump and laser modes inside the crystal at different pump power levels. The experiment was conducted with the 3 % output coupler. As shown in Fig. 4a, the thermal lensing became stronger with the increase of the pump power for both polarizations.

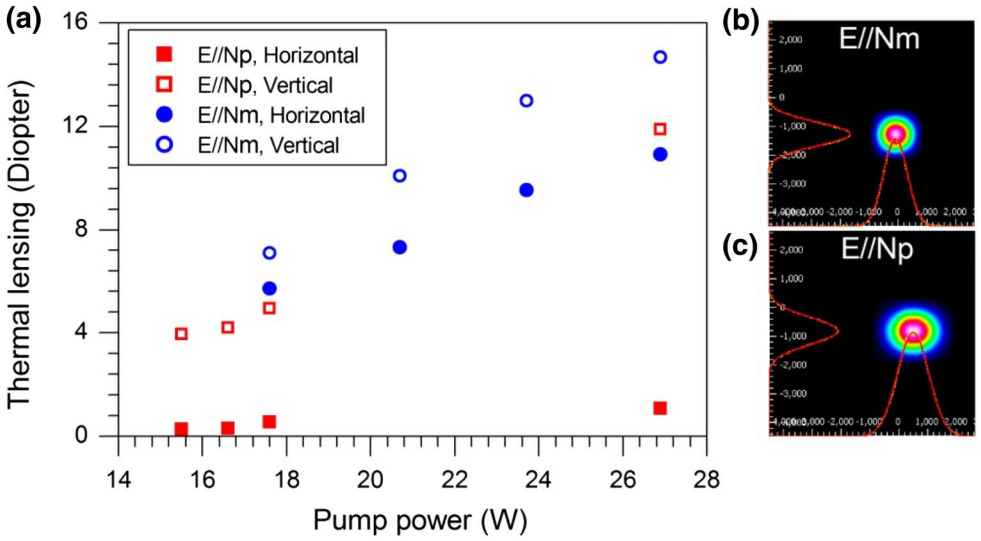

Fig. 4 The strength of thermal lensing as a function of the pump power (**a**) and the reshaped laser modes with the N_m-polarization (**b**) and N_p-polarization (**c**)

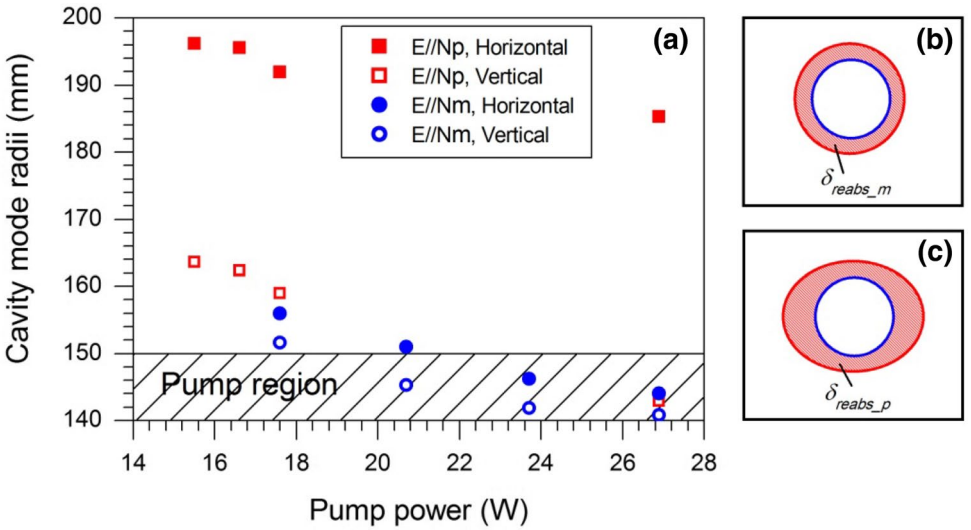

Fig. 5 Comparison of the size of the laser and the pump modes at different pump powers (**a**), the schemes of the spatial mismatching between the pump and laser modes for the N_m-polarization (**b**), and N_p-polarization (**c**). In **b**, **c,** the *inner circles* schematically depict the pump spots and *outer shapes* depict the laser modes

However, its strength exhibited a strong anisotropy which depended not only on the polarization but also on the direction considered. For the N_p-polarized mode, the sensitivity factors were estimated to be 0.1 m^{-1}/W for the horizontal direction and 0.95 m^{-1}/W for the vertical direction, with the astigmatism degree of 0.85 m^{-1}/W, while in contrast for the N_p-polarized mode, the sensitivity factors were estimated to be 0.71 m^{-1}/W for the horizontal direction and 1.03 m^{-1}/W for the vertical direction, with the astigmatism degree of 0.32 m^{-1}/W. These values are in good agreement with the previous results [21, 22]. As a consequence, the laser modes were reshaped as shown in Fig. 4b, c. Considering the thermal lensing effect, the laser mode inside the gain medium can be traced through the ABCD matrices analysis. Figure 5a shows the estimated sizes of the laser modes inside the gain medium. At low pump power levels, both the N_m- and N_p-polarized modes were less affected by the thermal lensing, resulting in a larger mode size compared to the pump mode. More importantly, they were reshaped differently due to the anisotropic thermal lensing, which in particular had a very weak effect on the horizontal direction of the N_p-polarized mode. Figure 5b, c schematically depicts the mismatch between the pump mode and the N_m- and N_p-polarized modes at the central plane of the crystal. Apparently, the N_p-polarized mode suffered different reabsorption loss in the unpumped region than the N_m-polarized mode at the same pump power level. As the pump power was increased, both laser modes and hence the reabsorption losses were reduced.

The net gain for the N_m- and N_p-polarized laser modes can be expressed as the following:

$$g_{n\_m}(\lambda_m) = g_m(\lambda_m) - \delta_{reabs\_m} \quad (1)$$

$$g_{n\_p}(\lambda_p) = g_p(\lambda_p) - \delta_{reabs\_p}, \quad (2)$$

where $g_m(\lambda_m)$ and $g_p(\lambda_p)$ are the gains for the N_m- and N_p-polarized laser modes at their lasing wavelengths λ_m and λ_p when they are spatially well matched with the pump mode, and δ_{reabs_m} and δ_{reabs_p} are the additional reabsorption losses in the unpumped regions of the crystal. It should be noted that the reabsorption in the pumped regions has been taken into account in the $g_m(\lambda_m)$ and $g_p(\lambda_p)$. The peak positions and values of the g_m and g_p are determined by the population inversion level N_u/N, where N_u is the ion concentration at the excited energy level and N is the doping concentration. It can be estimated that at $N_u/N = 13.2$ %, the g_m and g_p have the same values, corresponding to the emission wavelength $\lambda_m = 1028.5$ nm for the N_m-polarized mode and $\lambda_p = 1037.7$ nm for the N_p-polarized mode. At low inversion levels $N_u/N < 13.2$ %, the N_p-polarized mode has a higher gain $g_p(\lambda_p)$ than the $g_m(\lambda_m)$ for the N_m-polarized mode. Therefore, the N_p-polarized mode would play a dominant role if no special measures are taken. In the present lasing configuration, however, the dynamic variation of the reabsorption loss in the unpumped region of the crystal with the pump power helped to equalize the net gains of both laser modes.

At the threshold pump power level, both the N_m- and N_p-polarized modes were weakly focused by the thermal lensing in the gain medium and therefore experienced high reabsorption losses. According to the lasing wavelength of 1037.9 nm for the N_p-polarized mode, the inversion level N_u/N and the gain g_p were estimated to be 11.3 % and 0.058 [19]. At this inversion level, the gain g_m for the N_m-polarization should be around 0.05. Although the N_p-polarized mode suffered higher reabsorption loss δ_{reabs_p}, its larger gain g_p at the lasing wavelength made its net gain g_{n_p} still higher when compared to that one of the N_m-polarized mode g_{n_m} (i.e., $g_{n\_p} > g_{n\_m}$). Therefore, only the N_p-polarized mode oscillated in the cavity at this power level. The increase of the pump power allowed the N_m-polarized mode to be focused to smaller dimensions (due to stronger thermal lensing, see Fig. 4), leading to a reduction of the reabsorption loss δ_{reabs_m} and thus an increase in its net gain g_{n_m}. As the pump power was increased to 16.6 W (for the 3 % output coupler), g_{n_m} was increased to a level comparable to the net gain of the N_p-polarized mode g_{n_p} (i.e., $g_{n\_p} \approx g_{n\_m}$). This equalized gain allowed both of the N_m- and N_p-polarized modes to oscillate in the cavity and started their competition as pump power was further increased. Due to the stronger thermal lensing effect for the N_m-polarized mode, it experienced larger reduction of the reabsorption loss than the N_p-polarized mode at higher pump power levels. This allowed the N_m-polarized mode to overtake the N_p-polarized mode in the net gain competition and to become the dominant oscillating mode as the pump power was further increased to 18.6 W.

At higher pump power levels (>20.7 W), the N_m-polarized mode was focused to a dimension similar to the pump mode, making its reabsorption loss in the unpumped region to reduce to a very low value close to zero. As a consequence, the gain of the N_m-polarized mode would no longer suffer additional losses, that is, the net gain was increased to its maximum value of g_m (i.e., $g_{n\_m} = g_m$). In contrast, the net gain of the N_p-polarized mode g_{n_p} would continue to increase with the increase of the pump power due to thermal lensing. This allowed the g_{n_p} reaching to a level comparable to the g_m, therefore leading to the second coexistence of both the N_m- and N_p-polarized modes. As the g_{n_p} exceeded the g_{n_m} at higher pump power levels, the N_p-polarized mode again played the dominant role and even fully suppressed the N_m-polarized mode at higher pump power. In this gain equalization process, however, the reduction of the reabsorption loss δ_{reabs_p} and thus the increase of the net gain g_{n_p} for the N_p-polarized mode were less sensitive to the pump power (mainly because of the weak effect thermal lensing on its horizontal direction), therefore allowing the coexistence of the N_m- and N_p-polarized modes to be observed in a broader pump power range until the balance was fully broken at the pump power of 26.8 W. At this power level, the laser was linearly polarized along the N_p-axis as $g_{n\_p} > g_{n\_m}$.

For the 5 % output coupler (Fig. 2c), the reappearance of the N_p-polarized mode occurred at a higher pump power (24.8 W) than for the other output couplers. This can be attributed to the nonoptimized position of the end HR mirror during the translation, which plays an important role in the control of the spatial mismatch between the pump and laser modes and thus the reabsorption loss in the unpumped region of the crystal. Translation of the HR mirror farther away from the concave mirror R3 could help to reduce the laser mode sizes in the crystal. Therefore, a lower pump power (and thus a weaker thermal lensing effect) would be required to shrink the laser modes to the appropriate sizes in order to achieve equalized net gain for polarization switching. Under the current conditions, the second complete switching between the N_m- and N_p-polarized modes can be expected at higher pump power levels.

It is worth noting that since the strength of the thermal lensing depends on the pump power, the laser mode sizes and hence the introduced reabsorption losses are also power-dependent. Therefore, using the presented polarization-dependent reabsorption loss as a mechanism to reach gain equalization, the dual-wavelength operation can be controlled by the pump power and achieved in certain pump power ranges. In addition, as can be seen from Fig. 2, the ratio of the output powers at both wavelengths depended on the pump power. This indicates that the output power ratio can be also controlled by adjusting the pump power. In our experiments spectral intensities of both wavelengths were

stable within 10–20 % depending on the pump power and output coupling level.

More accurate analysis of the net gain equalization between the N_m- and N_p-polarized modes can be accomplished with the quantitative knowledge of the transverse and longitudinal inhomogeneity of the pump and laser modes, the temperature-dependent absorption and emission cross sections, and the spatial variation of the gain along the gain medium [23, 24]. With the flat reflectivity curve in the 1010- to 1100-nm range, we believe that the intracavity HR optics had negligible effect on the equalization of the gain at different wavelengths. Likewise, the variation of reflectivity for each output coupler in the observed lasing wavelength range (<0.1 %) had negligibly small and constant effect on the net gain of both polarizations, therefore having little contribution to their dynamic competition with the increase of the pump power. Further investigation of the lasing dynamics for both polarizations would be helpful in the output power stabilization.

4 Conclusion

In conclusion, we reported on the simultaneous dual-wavelength lasing from two orthogonal polarizations of a continuous wave Yb:KGW oscillator. The gain equalization between the two lasing wavelengths was realized by introducing additional polarization-dependent reabsorption loss, which originated from the anisotropic thermal lensing effect leading to the reshaping of the laser modes. Therefore, dual-wavelength lasing was obtained in a simple cavity without using any additional intracavity wavelength- or polarization-dependent optical elements. As the pump power was increased, the dual-wavelength lasing occurred within two power ranges. This unique feature has not been observed in other solid-state oscillators before. Moreover, the dual-wavelength emission was demonstrated with varied output coupler transmissions, resulting in a modest tunability of the two lasing wavelengths as well as their spectral spacing. We believe that the effect of polarization-dependent thermal lensing can be potentially employed to achieve dual-wavelength operation in other crystal orientations (e.g., N_p-cut crystals) and many other laser materials with anisotropic lasing and thermal properties. As a note of proof, after initial report of our results in [25], a similar thermal lens-driven polarization switching in dual-wavelength operation was also observed in Tm:KL$(WO_4)_2$ laser [26]. However, the polarization switching in [26] occurred in a much narrower power range and resembled operation observed in previous works [10–17], since one of the laser modes quickly became unstable and was not supported due to the strong thermal lensing effect at high power levels.

Acknowledgments This work was supported by the Natural Sciences and Engineering Research Council of Canada, University of Manitoba, and Western Economic Diversification Canada.

References

1. Y.F. Chen, Appl. Phys. B **70**, 475–478 (2000)
2. K. Lünstedt, N. Pavel, K. Petermann, G. Huber, Appl. Phys. B **86**, 65–70 (2007)
3. B. Wu, P.P. Jiang, D.Z. Yang, T. Chen, J. Kong, Y.H. Shen, Opt. Express **17**, 6004–6009 (2009)
4. Y.P. Huang, C.Y. Cho, Y.J. Huang, Y.F. Chen, Opt. Express **20**, 5644–5651 (2012)
5. Y.Y. Lin, S.Y. Chen, A.C. Chiang, R.Y. Tu, Y.C. Huang, Y.F. Chen, Y.H. Chen, Opt. Express **14**, 5329–5334 (2006)
6. R.M. Woodward, B.E. Cole, V.P. Wallace, R.J. Pye, D.D. Arnone, E.H. Linfield, M. Pepper, Phys. Med. Biol. **47**, 3853–3863 (2002)
7. K. Kawase, Y. Ogawa, Y. Watanabe, H. Inoue, Opt. Express **11**, 2549–2554 (2003)
8. T.G. Phillips, J. Keene, Proc. IEEE **80**, 1662–1678 (1992)
9. A.N.P. Bustamante, D.A. Hammons, R.E. Peale, B.H.T. Chai, M. Richardson, A. Chin, Opt. Commun. **192**, 309–313 (2001)
10. J.H. Liu, X. Mateos, H.J. Zhang, J.Y. Wang, M.H. Jiang, U. Griebner, V. Petrov, Opt. Lett. **31**, 2580–2582 (2006)
11. J. Liu, H. Zhang, J. Wang, V. Petrov, Opt. Lett. **32**, 2909–2911 (2007)
12. J. Liu, H. Yang, H. Zhang, J. Wang, V. Petrov, Appl. Opt. **47**, 5436–5441 (2008)
13. A. Brenier, C. Tu, Z. Zhu, J. Li, Appl. Phys. B **89**, 323–328 (2007)
14. R. Czarny, M. Alouini, C. Larat, M. Krakowski, D. Dolfi, Electron. Lett. **40**, 942–943 (2004)
15. A. Brenier, Laser Phys. Lett. **8**, 520–524 (2011)
16. F. Druon, M. Olivier, A. Jaffrès, P. Loiseau, N. Aubry, J. Didier-Jean, F. Balembois, B. Viana, P. Georges, Opt. Lett. **38**, 4138–4141 (2013)
17. J.M. Serres, P. Loiko, X. Mateos, K. Yumashev, N. Kuleshov, V. Petrov, U. Griebner, M. Aguiló, F. Díaz, Opt. Mater. Express **5**, 661–667 (2015)
18. R. Akbari, H. Zhao, A. Major, Opt. Lett. **41**, 1601–1604 (2016)
19. H. Zhao, A. Major, Opt. Express **22**, 26651–26658 (2014)
20. H. Mirzaeian, S. Manjooran, A. Major, Proc. SPIE **9288**, 928802 (2014)
21. G.H. Kim, J. Yang, B. Lee, E.G. Sall, S.A. Chizhov, V.E. Yashin, U. Kang, Quantum Electron. **45**, 211–215 (2015)
22. P.A. Loiko, I.A. Denisov, K.V. Yumashev, N.V. Kuleshov, A.A. Pavlyuk, Appl. Phys. B **100**, 477–483 (2010)
23. S. Yiou, F. Balembois, P. George, J. Opt. Soc. Am. B **22**, 572–581 (2005)
24. B. Jacobsson, J.E. Hellström, V. Pasiskevicius, F. Laurell, Opt. Express **15**, 1003–1010 (2007)
25. H. Zhao, A. Major, in CLEO: 2013, OSA Technical Digest Series (OSA, 2013), P. CTh4I.2
26. P.A. Loiko, X. Mateos, N.V. Kuleshov, A.A. Pavlyuk, K.V. Yumashev, V. Petrov, U. Griebner, M. Aguilo, F. Diaz, IEEE J. Quantum Electron. **50**, 669–676 (2014)